CFD Investigation of Slurry Seawater Flow Effect in Steel Elbows

A. I. Shahata[1], M. Talaat Youssef[1], Khalid Saqr[1] and Mohamed Shehadeh[2*]

[1]*Mechanical Engineering Department, Arab Academy for Science, Technology and Maritime Transport, Alexandria, Egypt*
[2]*Marine Engineering Department, Arab Academy for Science, Technology and Maritime Transport, Alexandria, Egypt*

Abstract

This paper is concerned with studying the erosion rates due to both flow rate variations as well as sand concentration variations. The flow rate was controlled to cover both the laminar and turbulent flow regimes. The laminar and turbulent regimes are ranging from 580 to 2200 and from 5000 to 26000 respectively. The sand concentration varied from 1 up to 11 grams per litre. Discrete Phase Model (DPM) is developed using general purpose CFD code. The grid independency study is constructed and the model is verified with laboratory experiments. The relationship between the erosion rate of steel and flow rate at different levels of contamination is correlated. A model for predicting erosion-corrosion rate for laminar and turbulent flow regimes for different sand contamination levels is presented.

Keywords: *CFD; Erosion model; Slurry Seawater; erosion–corrosion.*

1. Introduction

Contaminants in seawater are a major cause for erosion-corrosion phenomena. Erosion-corrosion is characterized in appearance by grooves, gullies, waves, rounded holes and usually exhibits a directional pattern [1]. The motion is usually one of high velocity, with mechanical wear and abrasion effects. Flow velocities influence the erosion behaviour, when the velocity of the flow increases the rate of erosion-corrosion increase [2]. The erosion-corrosion behaviour is affected by many parameters such as the flow velocity and the solid-particle contaminant concentration [3]. The flow velocity is widely studied because of its influence on the design process of fresh/sea water systems subjected to corrosion effects.

Mohyaldin et. al. [4] studied three different modelling methods used for erosion prediction in pipe components due to sand production with oil and gas. The study was comparison between Salama model [13] (i.e. empirical), DIM (i.e. semi-empirical) , and DPM model (i.e. CFD) ,The result of the study was in fair agreement of the DIM model with the CFD with an overall error of 10%, whereas Salama model highly overestimates the CFD by nearly 150%.

Chen and S.Mclaury [5] studied the relative erosion severity between plugged tees and elbows in dilute gas/solid (i.e. two-phase flow). The numerical part was contacted using a CFD model to predict the erosive wear severity. The experimental part was conducted to verify the simulation results obtained for gas/sand flows. They stated that the ratio of erosion at the end of the plugged section to the elbow was nearly constant value at all conditions. Based on the analysis of the CFD simulations and experimental data, a constant value of 0.5 is recommended for relative erosion severity between the end region of plugged tees and elbows. Experiments under high sand volume concentration indicate that the erosion in plugged tees was about two orders of magnitude and less than erosion in elbows.

Abdolkarimi and Mohammadikhah, [6] studied the effect of particles size distribution on particles flow pattern and their erosive effect on the bend through the computational fluid dynamics modelling of solid particles hydrodynamic based on Lagrangian framework for diluted solid-gas flow through 90° gas pipeline bend. Also the erosion rate at the outer wall of the bend was predicted. The pipeline bend had a pipe diameter of 1422.4mm and ratios of the bend radius of the curvature to the pipeline diameter of 1.5. For the validation of computational model, at first the computational modelling is performed for a published

experimental solid-gas flow data. The computational results include radial gas velocity and radial particle velocity profiles on planes which are at different angles through the bend. The comparison between predicted numerical results with similar experimental data proves that the predictions of computational model are acceptable. The experimental work data exceeds the numerical one by 27%. Finally the particles size distribution on each plane through the bend and the erosion rate on the outer wall of the bend have been obtained. The maximum rate of erosion is found to be 3.2 nm/s. This paper was considered in the validation section. The current paper introduces the model description including numerical model, model geometry and meshing, grid dependency study, numerical scheme selection and model validation. Also, the current work presented a case study showing the variation of the solid contents mass and how it influences the erosion rate.

2. Model description

2.1. Numerical Model

Numerically, discrete phase model is used to model multiphase flows in the FLUENT. The problem is to build a valid model with acceptable results.The flow is governed by the Navier-Stokes equations. The continuity equation is given by,

$$\rho \frac{\partial U_i}{\partial x_i} = 0 \tag{1}$$

The momentum equation for incompressible flow is given by,

$$\rho U_i \frac{\partial U_j}{\partial x_i} = -\frac{\partial P}{\partial x_i} + \left(\mu \left(\frac{\partial^2 U_i}{\partial x_j 2} + \frac{\partial^2 U_j}{\partial x_i \partial x_j} \right) - \rho \overline{u_j u_i} \right) \tag{2}$$

Where $\rho \overline{u_j u_i}$ = 0 for laminar flow

The energy equation is given by:

$$\nabla(\mu(E + p)) = 0 \tag{3}$$

In the k- ε turbulence model, the unknown Reynolds stresses, $\overline{u_j u_i}$, are assumed to vary linearly with the local strain rates as eddy viscosity (v_t) is evaluated from

$$v_t = c_\mu \frac{k^2}{\varepsilon} \tag{4}$$

The program predicts the trajectory of a discrete phase particle (or droplet or bubble) by integrating the force balance on the particle, which is written in a Lagrangian reference frame. This force balance equates the particle inertia with the forces acting on the particle, and can be written (for the x direction in Cartesian coordinates) as

$$\left(\frac{\mathrm{dup}}{\mathrm{dt}}\right) = (\mathrm{FD})\big((\mathrm{u}) - (\mathrm{up})\big) + (\mathrm{gx})\frac{(\rho \mathrm{p}) - (\rho)}{\rho \mathrm{p}} \tag{5}$$

The drag force imposed on the particles is given by equation (6)

$$(\mathrm{FD}) = \frac{18\mu}{\rho \mathrm{p}(d\mathrm{p})^2} * \frac{CD}{24}\big((\mathrm{u}) - (\mathrm{up})\big) \tag{6}$$

Where:

$$(CD) = (a1) + \frac{a2}{Re} + \frac{a3}{Re^2} \tag{7}$$

And:

$$(Re) = \frac{\rho d\mathrm{p}}{\mu} * |\ (\mathrm{u}) - (\mathrm{up})\ | \tag{8}$$

The erosion rate is defined as

$$ER = \sum_{P=1}^{N:\ no\ of\ particles} m\,\dot{C}(d_p)\frac{f(\propto)v^{b(v)}}{Area_{Face}} \tag{9}$$

Where C (dp) is a function of particle diameter, $\propto$ is the impact angle of the particle path with the wall face, f ($\propto$) is a function of impact angle, v is the relative particle velocity, b (v) is a function of relative particle velocity, and Aface is the area of the cell face at the wall. Default values are C = 1.8 * 10^-9, f = 1, and b = 0.The erosion rate is computed assuming reflecting wall boundary condition. For steel material n=2.6, Fs=0.2 (for fully rounded solid particles).

2.2 Model Geometry

In our case a study was held on a 50.2 mm long radius carbon steel elbow 90 degree with internal diameter 50.8 mm.

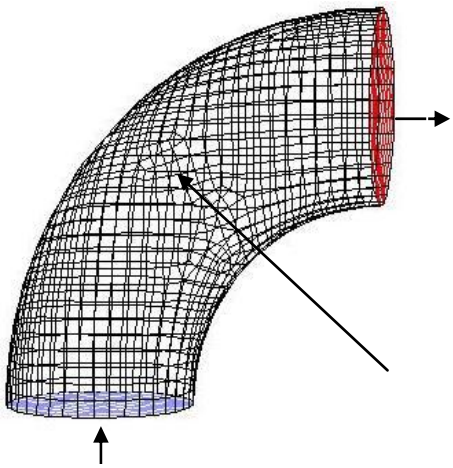

Figure 1. Model geometry and faces

The model is meshed using GAMBIT and we obtained 4 sets of meshed Quad symmetric cells. The number of meshed cells is listed in the table 1.

Table 1.Model meshing sets details

Mesh ID	Number of Meshed Cells	Number of faces	Number of nodes
A	1969	4194	523
B	10909	22777	2500
C	102961	211373	20913
D	**77564**	**159244**	**15755**

2.4. Grid independency study

Here we study the radial velocity distribution along the elbow diameter for the four meshed sets. From the graph presented we chose the [D] set for the perfect solution

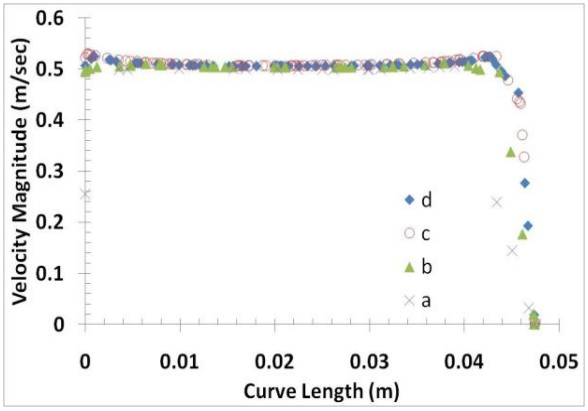

Figure 2. Velocity horizontal magnitude distribution along the elbow curve length

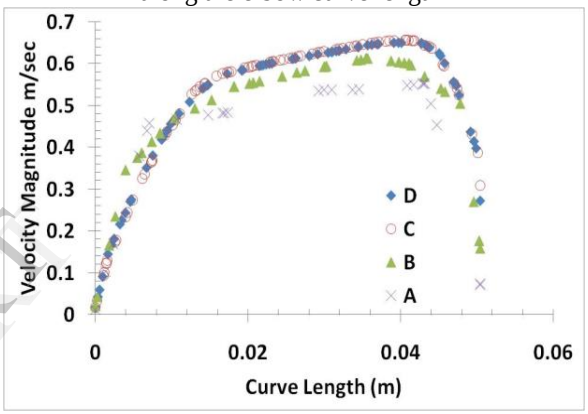

Figure 3. Velocity vertical magnitude distribution along the elbow curve length

2.5 Numerical Scheme selection

In this process, the main aim is to select the most accurate numerical scheme after a complete comparison between all the schemes to reach a proper value considering the computational cost.. After the grid independency study made and the selection is the [D] set, numerical scheme sets are computed. The following charts show the radial velocity distraction at all the indicated numerical schemes. After comparing every output value with the outlet velocity facet average value 0, the most proper value was related to standard K – ω turbulence model.

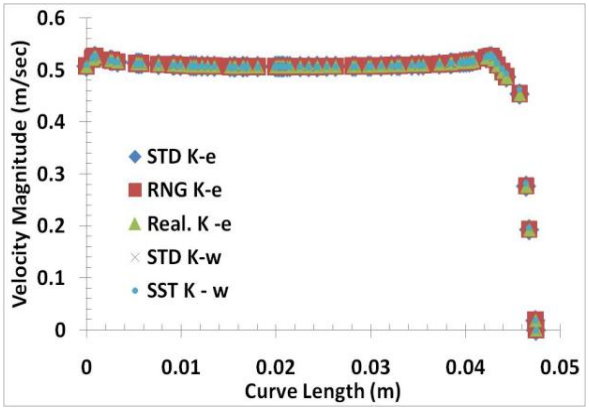

Figure 4. Velocity horizontal magnitude distribution along the elbow curve length

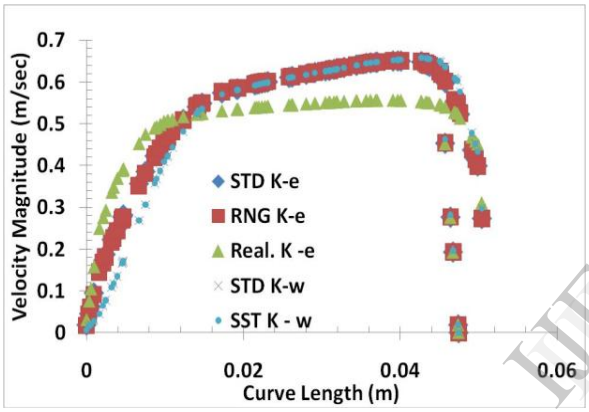

Figure 5. Velocity vertical magnitude distribution along the elbow curve length

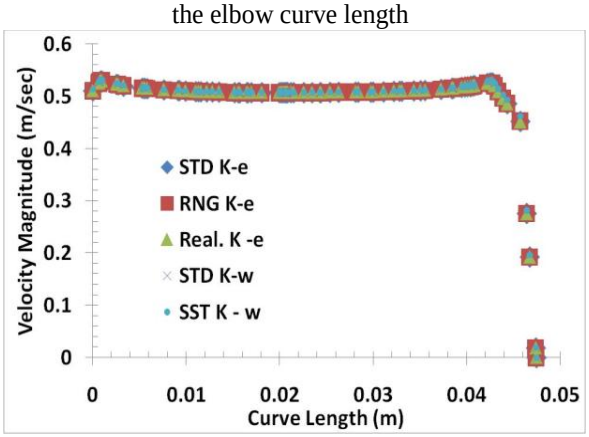

Figure 6. Velocity horizontal magnitude distribution along the elbow curve length

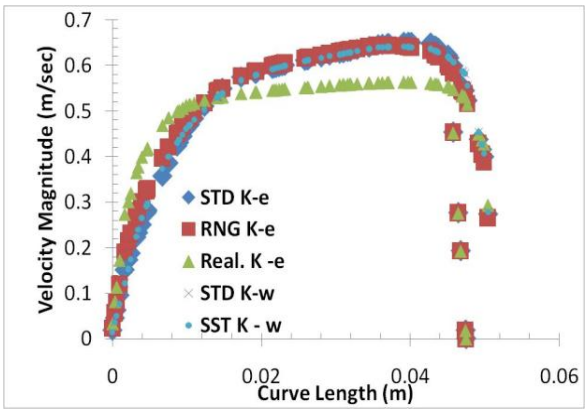

Figure 7. Velocity vertical magnitude distribution along the elbow curve length

2.6 Model Validation

In order to validate the model, The CFD results were compared to experimental measurements.

-Case I

Chen and S.Mclaury studied the relative erosion severity between plugged tees and elbows in dilute gas/solid two-phase flow through numerical and experimental investigations. The work was held experimentally with 1 inch long radius elbow for three air velocities: 15.72 m/sec , 30.48, and 45.42 m/sec. The relative plugged length (L/D) of the plugged tee is equal to 1.5. The erosion rate is estimated by using the material mass loss.

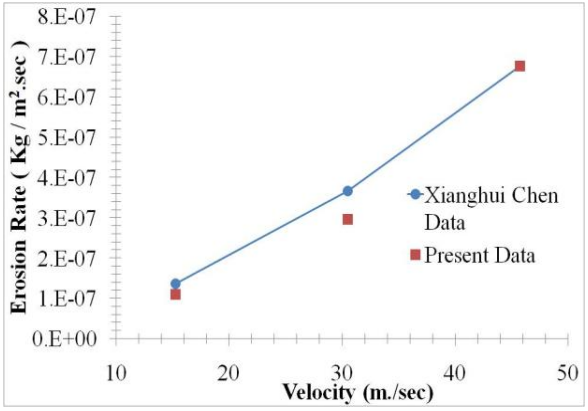

Figure 8. Xiangui Chen experimental elbow erosion rate data versus present DPM model.

The comparison between the experimental work and the present numerical model revealed that the model gave results with an approximate error of 12% compared to the experimental ones. The second comparison was between the experimental plugged tees erosion rate with respect to the numerical erosion rate as shown in Figure 8.

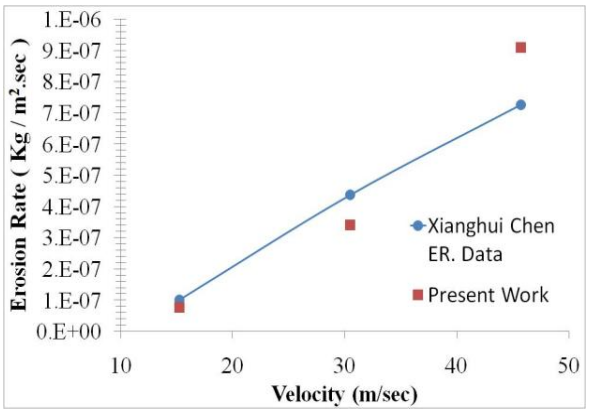

Figure 9. Xiangui Chen experimental Tee Plugged erosion rate data versus present DPM model.

The comparison between the experimental work and the present numerical model revealed that the model gave results with an approximate error of 24% compared to the experimental ones.

-Case II

Abdolkarimi et. al [6], modelled particles erosive effects on a commercial scale pipeline bend. The model showed that the maximum erosion obtained in the case was 2.63E-12 Kg/m2.sec and it will occure at an angle between 40 ° and 65 °. The DPM model showed it as 2.37E-12 Kg/m2.sec. The maximum difference was around 10%. The maximum erosion location was calculated by identifying the maximum erosion point on the contour graphically and it was found to be 41.7 ° which means that the present model made a good agreement with Vahid Abdolkarimi et. Al.

-Case III

Shehadeh,et. al [7], presented a study concerned with studying the behaviour of steel elbows working in erosive environments. Rates of iron losses due to both flow rate variations as well as sand concentration variations were investigated. A spectrophotometer was utilized to measure the quantity of iron losses. The relationship between the rate of iron loss and flow rate at different levels of contamination was studied. Figure 10 reveals a comparison between the experimental data with the DPM model. The DPM model showed good agreement with the experimental work with an overall error of 28%.

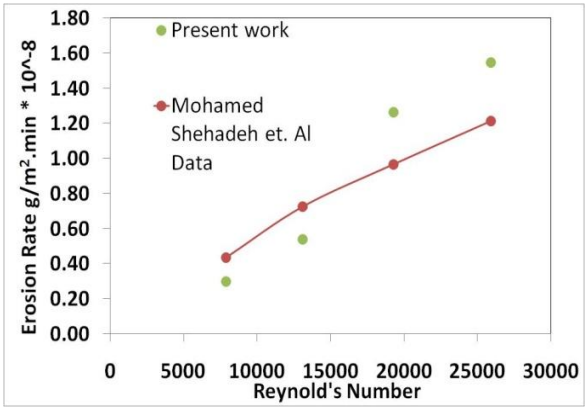

Figure 10. Shehadeh experimental elbow erosion rate data versus present DPM model.

3. Case Study

The Reynolds number calculations were based on the elbow inner diameter. The fluid used was seawater and its density and dynamic viscosity were taken as 1025 kg/m^3 and 0.0011 kg/ms, respectively[8].Sand of average grain size of 300 μm was added to the seawater injection at different concentrations. Boundary conditions are listed clearly at table 2.

Table 2. Boundary conditions

Injected Particle Type	Sand
Particle Density (kg.m^3)	1900
Particle Concentration (g/l)	• Case a: Seawater with 1 g/l sand concentration • Case b: Seawater with 5 g/l sand concentration • Case c: Seawater with 7 g/l sand concentration • Case d: Seawater with 8 g/l sand concentration • Case e: Seawater with 11 g/l sand concentration
Reynolds numbers	582.68,1176.63(Laminar flow) 7878.79,13107.75,19296.48 ,25922.2 (turbulent flow)

4. Results and Discussions

The computational analysis was implemented after validating the model with Shehadeh et. al . Shehadeh et. al investigated three different flow (3, 6 and 9g/l). The analysis was carried out to determine the erosion rate using equation (9) for five different flow environments and to determine the location of maximum erosion rate. The five different flow environments are:

- Seawater with 1 g/l sand concentration
- Seawater with 5 g/l sand concentration
- Seawater with 7 g/l sand concentration
- Seawater with 8 g/l sand concentration
- Seawater with 11 g/l sand concentration

Different flow velocities accompanied with different degree of concentrations are investigated and erosion rate was computed in each case. Figure 10 and 11 shows the model results of laminar and turbulent flow. Figure 10 shows the erosion rate computations in the laminar zone with different degrees of concentrations.

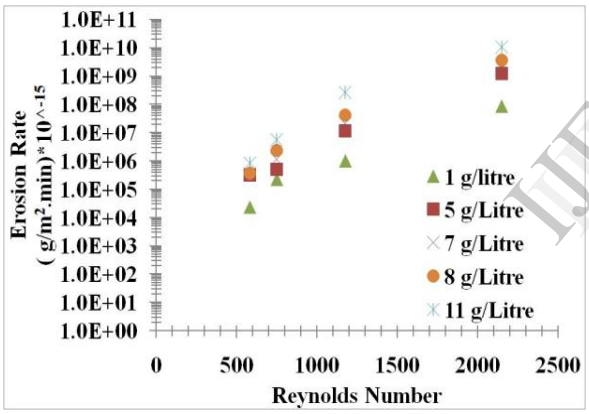

Figure 11. DPM erosion rate data for laminar flow

Figure 11 shows that there is an increment of the erosion rate with the increase of Reynolds number (i.e. increase of the velocity). Also the erosion rate increases with the particles concentration increase.

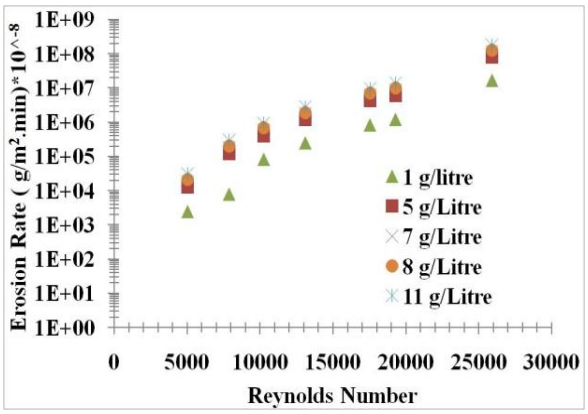

Figure 12. DPM erosion rate data for turbulent flow

Figure 12 shows that there is an increment of the erosion rate with the increase of Reynolds number (i.e. increase of the velocity). Also, the erosion rate increase with the increase of Reynolds's as well as increases with the particles concentration. From Figures (10), it is a clearly observed that erosion rate increases rapidly at changing the flow regime from laminar to turbulent, see Figure (12). Also, the location of maximum erosion rate at different velocities is considered. Figures 13 and 14 show the model results of laminar and turbulent flow for maximum erosion rate. The second objective is to allocate the maximum erosion rate. For example in the case of having Reynolds number 25922.2, the maximum erosion rate will occur at 63 ° as shown in Figure 15

.

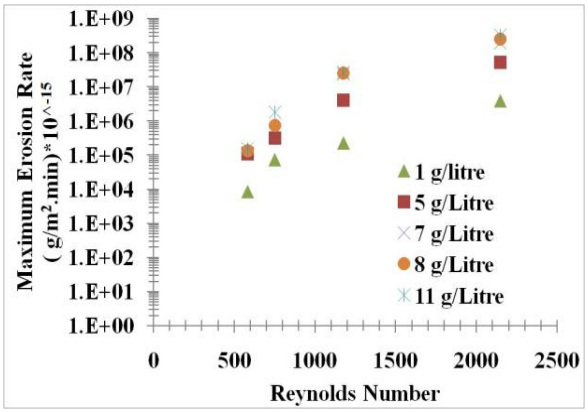

Figure 13. DPM Maximum erosion rate data for laminar flow

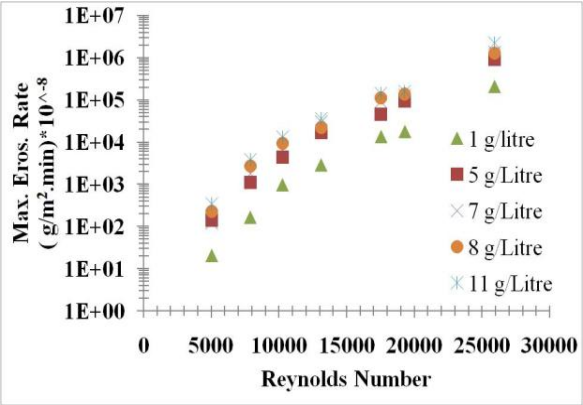

Figure 14. DPM Maximum erosion rate data for turbulent flow

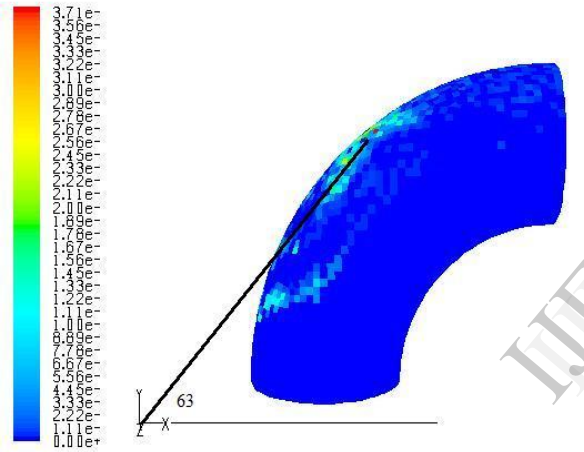

Figure 15. DPM Maximum erosion rate location at Re = 25922.2.

6. Conclusions

In this work the effect of seawater flow rate accompanied with seawater contamination level on erosion rates was investigated. The computations were run to include both laminar and turbulent flow regimes.

- By analyzing levels of particle concentrations, and types of flow; it was found that the erosion rate increases with the increase of flow velocities and particle concentration levels as well.
- Complete change is observed in the erosion rate when we change the flow from laminar regime to turbulent one.
- Maximum erosion rate location can be allocated.

7. References

[1] Fontana, M.G., Corrosion Engineering. 3rd ed. USA: McGraw-Hill, 1986

[2] Roberge, Pierre R., Handbook of Corrosion Engineering. USA: McGraw-Hill, 2000.

[3] Yang, Y. and Cheng, Y.F., Parametric effects on the erosion–corrosion rate and mechanism of carbon steel pipes in oil sands slurry. Wear, 276–277, 2012, pp. 141–148.

[4]Mazumder, Quamrul H., Shirazi, S., McLaury, B., "Experimental Investigation of the Location of Maximum Erosive Wear Damage in Elbows", Journal of Pressure Vessel and Technology, vol. 130, no. 1,

[5] X. Chen, B.S. MClaury, S.A. Shirazi, Application and experimental validation of a computational fluid dynamics (CFD) based erosion prediction model in elbows and plugged tees, Comput. Fluids vol. 33, 2004, pp.1251–1272

[6] Vahid Abdolkarimi , Rasoul Mohammadikhah, CFD Modeling of particulates erosive effect on a commercial scale pipeline Bend, Process development department Research Institute of petroleum industry Tehran Iran.

[7] Mohamed Shehadeh, Hany Mourad, Mohammed Anany and Ibrahim Hassan , Experimental Study of Erosion-Corrosion Due to Slurry Seawater Flow in Steel Elbows. International Conference on Mechanical Engineering Research (ICMER2013), Kuantan, Pahang, Malaysia, July 2013.

[8] Guo, C.Q , Zhang, C.H. and Paidoussis, M.P, 'Modification of equation of motion of fluid-conveying pipe for laminar and turbulent flow profiles', Journal of Fluids and Structures, Vol 26, No 5, pp. 793-803.February 2008, pp. 31-38.

[9] Nayyar, M.L., Piping Handbook, 7th ed. USA: McGraw-Hill, 2000.

[10] M.M. Stack, N. Pungwiwat, Particulate erosion–corrosion of Al in aqueous conditions: some perspectives on pH effects on the erosion–corrosion map, Tribol. Int., vol. 35, 2002, pp.651–660.

[11] I. Finnie, Erosion of surfaces by solid particles, Wear 3, 1960, pp.87–103.

[12] S.A. Shirazi, J.R. Shadley, B.S. McLaury, E.F. Rybicki, A procedure to predict solid particle erosion in elbows and tees, J. Pressure Vessel Technol. 117, 1995, pp.45–52.

[13] M. Salama, An alternative to API erosional velocity limits for sand laden fluids, in: Proceedings of Offshore Technology Conference, Paper No. OTC-8898, Houston, TX, USA, 1998.

[14] Fluent 6.3 user guide, Fluent Inc., Lebanon. New-Hampshire,USA,Dec.2001.